Supporting Information

Influence of solution pH on degradation of atrazine during UV and UV/H_2O_2 oxidation: Kinetics, mechanism, and degradation pathways

Yucan Liu[a*], Kai Zhu[b*], Miaomiao Su[a], Huayu Zhu[c], Jianbo Lu[a], Yuxia Wang[d], Jinkun Dong[a], Hao Qin[a], Ying Wang[a] and Yan Zhang[a]

[a]School of Civil Engineering, Yantai University, Yantai 264005, China.

[b]College of resources and environment, Linyi University, Linyi 276000, China.

[c]School of chemistry & chemical engineering, Linyi University, Linyi 276000, China.

[d]School of Environmental and Municipal Engineering, North China University of Water Resources and Electric Power, Zhengzhou, 450046, China

Corresponding author:

Yucan Liu Ph.D.

School of Civil Engineering, Yantai University

30 Qingquan Road, Yantai, 264005, China

E-mail: liuyucan@ytu.edu.cn

Tel: +86 0535 6902606

Fax: +86 0535 6902606

Mobile: +86 15853588482

Kai Zhu Ph.D.

College of resources and environment, Linyi University

Shuangling Road, Linyi, 276000, China

E-mail: zhukai@lyu.edu.cn

Contents

Text S1 Parameters of UPLC and MS for identifying UV photo-oxidation products.

The binary mobile phase was composed of methanol (mobile phase A) and ultrapure water (mobile phase B), and the flow rate was 0.2 mL min^{-1}. The elution started with 10% A for 3 minutes, the concentration of A was increased to 70% within 18 minutes, and then the concentration of A was increased to 100% within 22 minutes and retained for 3 minutes, finally it was dropped back to 10% and run for 3 minutes for equilibrium before the next injection. A total acquisition time of one run analysis was 28 min. The column temperature was maintained at 35 ºC and the injection volume was 10 µL. The source temperature and desolvation temperature were 110 ºC and 350 ºC, the capillary voltage was 3.3 kV, and the cone voltage was 35 V. Desolvation gas (nitrogen gas) and cone gas (nitrogen gas) flows were set at 500 L h^{-1} and 30 L h^{-1}, respectively. Full scan data were acquired from *m/z* 50 to 300 at an acquisition rate of 0.2 sec $scan^{-1}$ in both positive electrospray ionization (ESI+) mode and negative electrospray ionization (ESI-) mode. In order to obtain further information for analyzing the structure of intermediates, collision induced dissociation (CID) experiments in daughter scan were also conducted. Argon was used as collision gas in daughter scan model and its flow rate was at 0.12 mL min^{-1}. The collision energy for each product was optimized in the range from 15 to 35 eV.

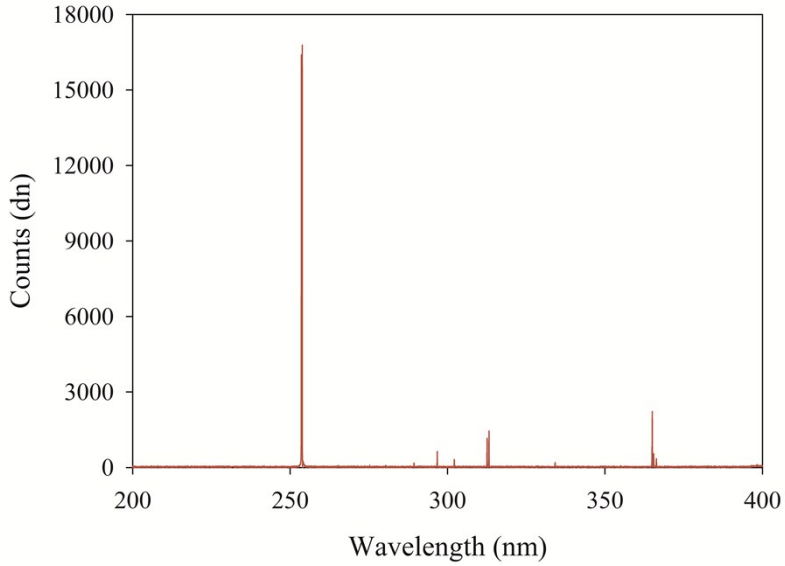

Fig. S1 Emission spectrum of the low-pressure mercury UV lamp.

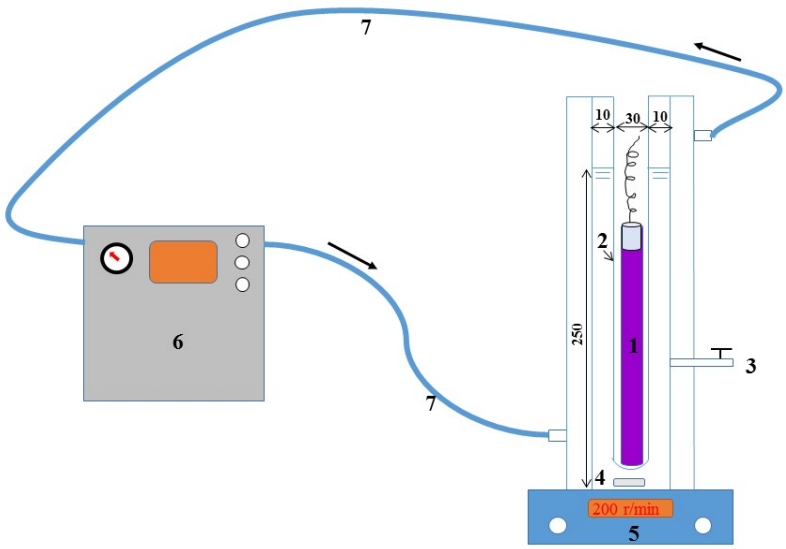

Fig. S2 Schematic diagram of photochemical reactor.

(1) low-pressure mercury UV lamp; (2) quartz glass well; (3) sampling point; (4) magnetic stirrer; (5) magnetic stirrer apparatus; (6) thermostatic water recirculation system; (7) silicone tube. All dimensions are in millimeter (mm).

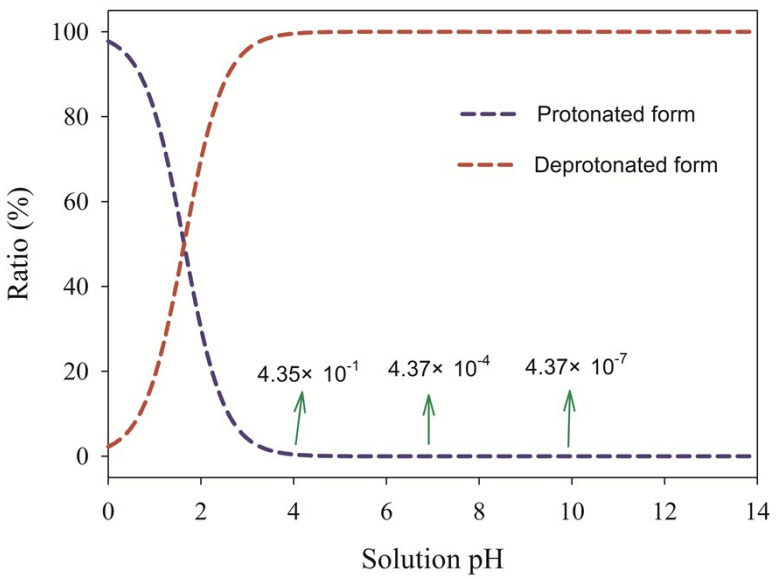

Fig. S3 Distribution for protonated and deprotonated ATZ species as a function of solution pH. $C_{Total} = C_{Deprotonated\ form} + C_{Protonated}$.

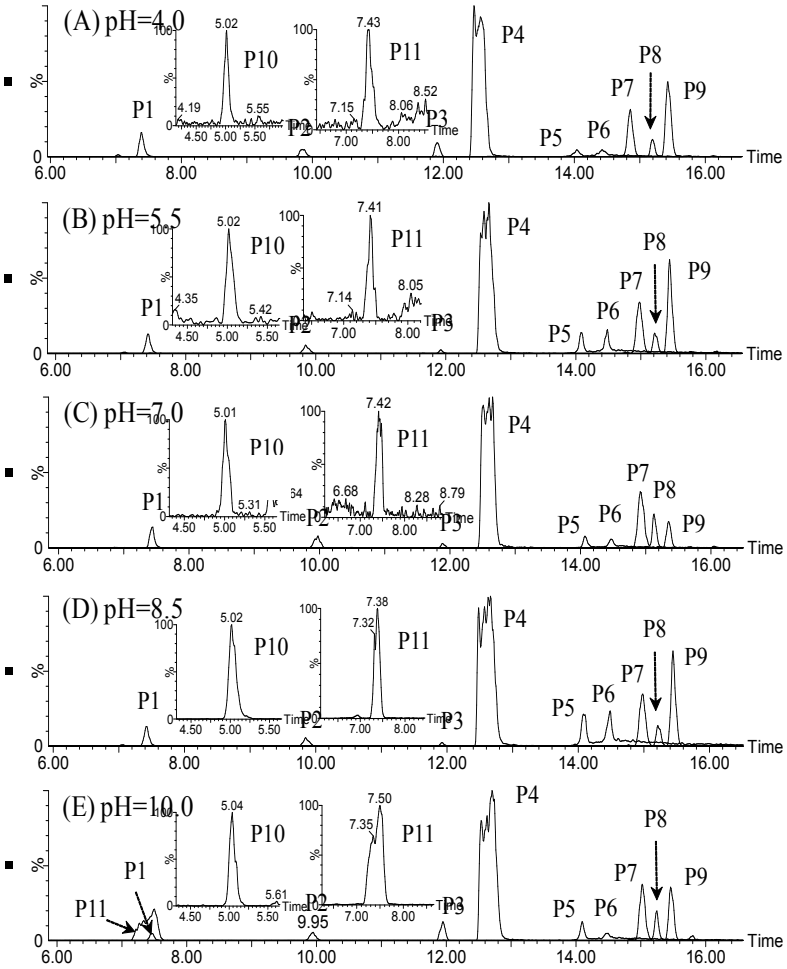

Fig. S4 The EIC of photo-degradation intermediates of ATZ in solution during sole-UV treatment. Raw ATZ solution: 5 mg L^{-1}; irradiation time: 120 min. (A) pH 4.0; (B) pH 5.5; (C) pH 7.0; (D) pH 8.5; (E) pH 10.0.

P1 (4-Isopropylamino-6-amino-*s*-triazine)

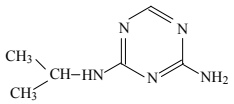

ESI+ mode

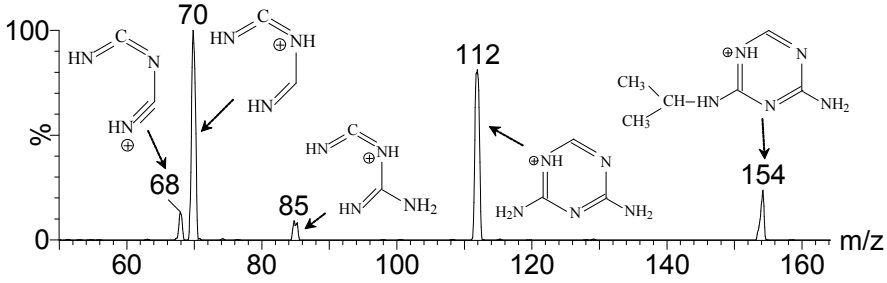

Fig. S5 Molecular structure and MS/MS spectrum of P1 (ESI+, CE=22 eV).

P2 (2-Methoxy-4-methylamino-6-isopropylamino-*s*-triazine)

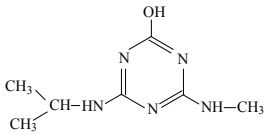

ESI+ mode

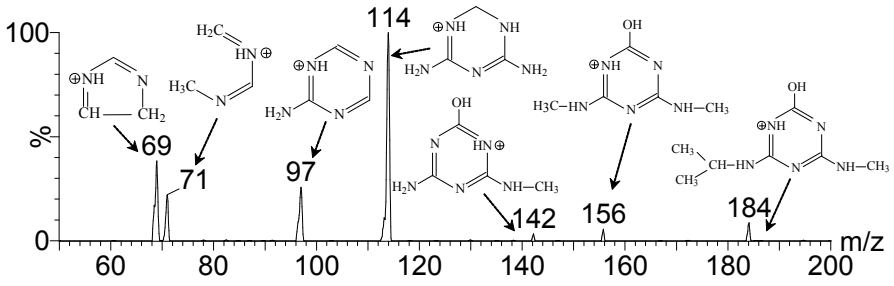

Fig. S6 Molecular structure and MS/MS spectrum of P2 (ESI+, CE=22 eV).

P3 (2-Hydroxy-4-isopropylamino-6-vinylamino-*s*-triazine)

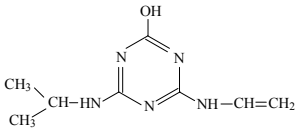

ESI+ mode

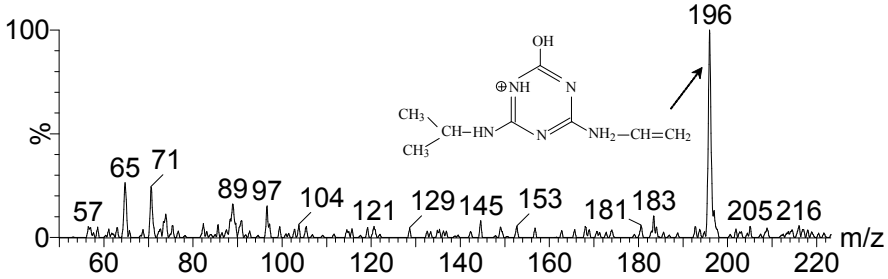

Fig. S7 Molecular structure and MS/MS spectrum of P3 (ESI+, CE=0 eV).

P4 (2-Hydroxy-4-ethylamino-6-isopropylamines-*s*-triazine)

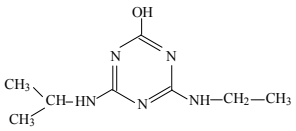

ESI+ mode

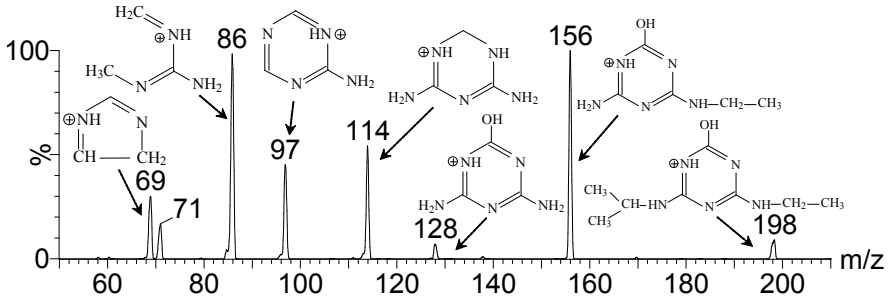

ESI- mode

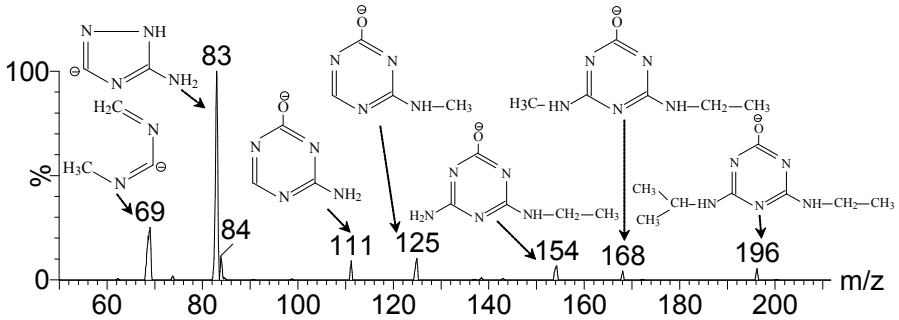

Fig. S8 Molecular structure and MS/MS spectrum of P4 (ESI+ and ESI-, CE=23 eV).

P5 (2-Hydroxy-4-acetamido-6-ethylamino-*s*-triazine)

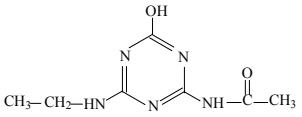

ESI+ mode

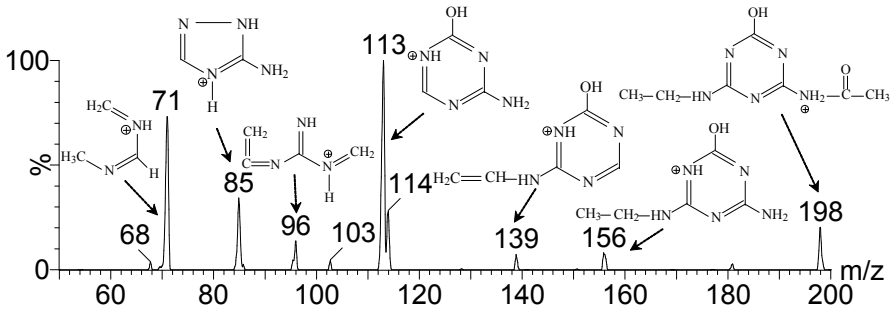

ESI- mode

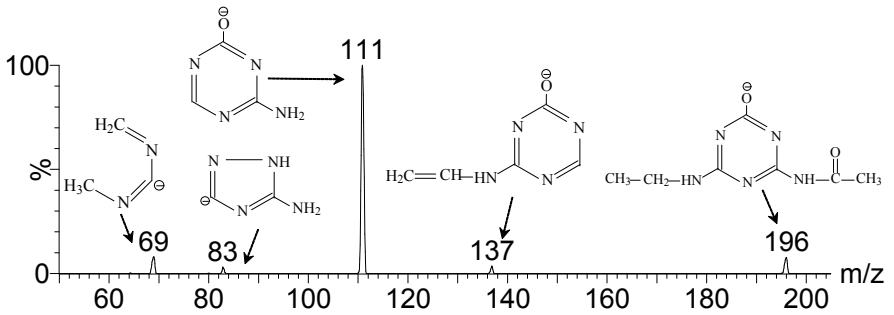

Fig. S9 Molecular structure and MS/MS spectrum of P5 (ESI+ and ESI-, CE=16 eV).

P6 (2-Hydroxy-4-(2-hydroxy-ethylamino)-6-vinylamino-*s*-triazine)

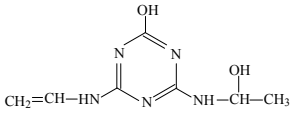

ESI+ mode

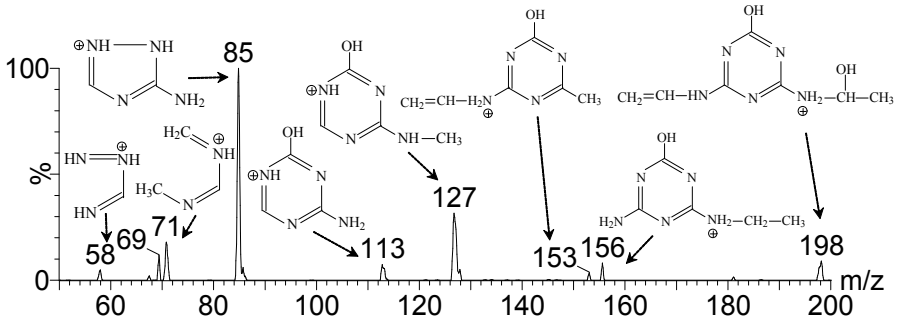

ESI- mode

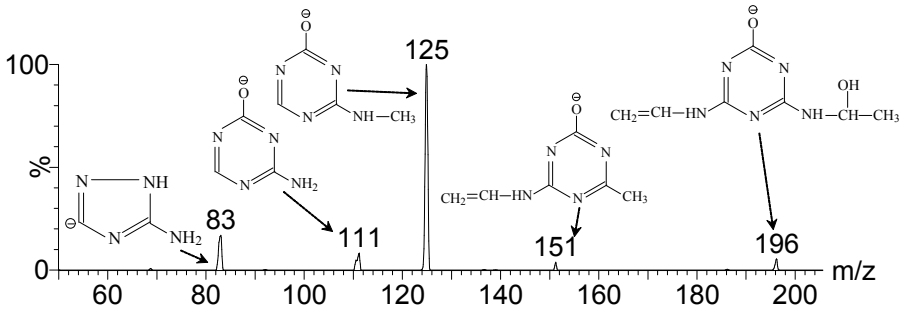

Fig. S10 Molecular structure and MS/MS spectrum of P6 (ESI+ and ESI-, CE=24 eV).

P7 (2-Hydroxy-4-acetamido-6-isopropylamino-*s*-triazine)

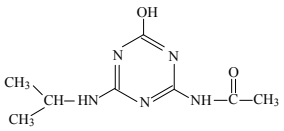

ESI+ mode

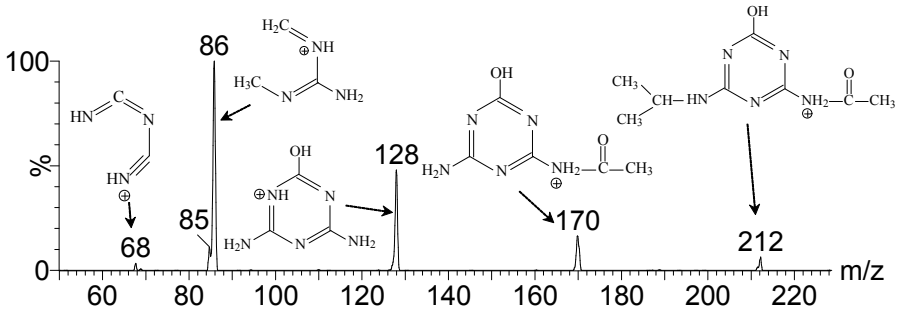

Fig. S11 Molecular structure and MS/MS spectrum of P7 (ESI+, CE=26 eV).

P8 (2-Methoxy-4-isopropylamino-6-ethylamino-*s*-triazine)

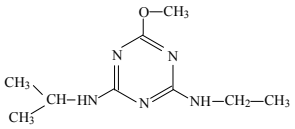

ESI+ mode

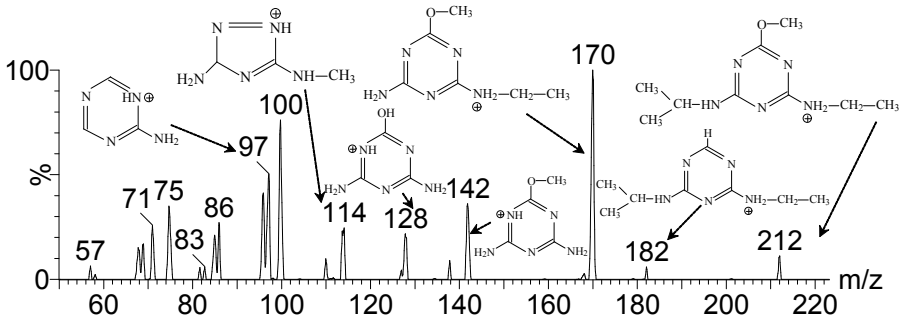

Fig. S12 Molecular structure and MS/MS spectrum of P8 (ESI+, CE=22 eV).

P9 (2-Chloro-4-ethylamino-6-isopropylamino-*s*-triazine)

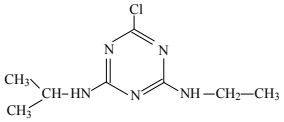

ESI+ mode

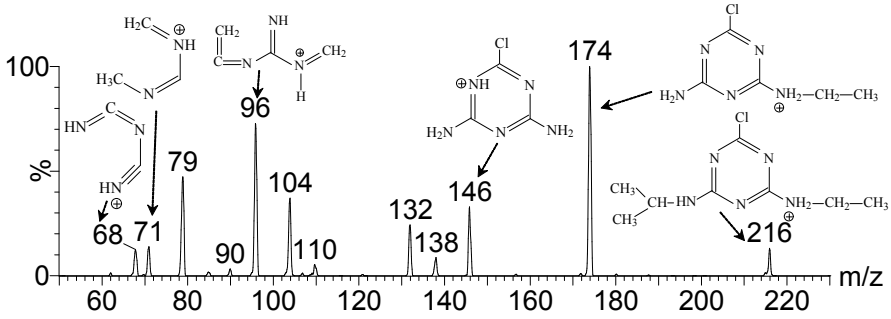

Fig. S13 Molecular structure and MS/MS spectrum of P9 (ESI+, CE=22 eV).

P10 (2-Hydroxy-4-vinylamino-*s*-triazine)

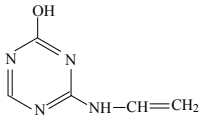

ESI+ mode

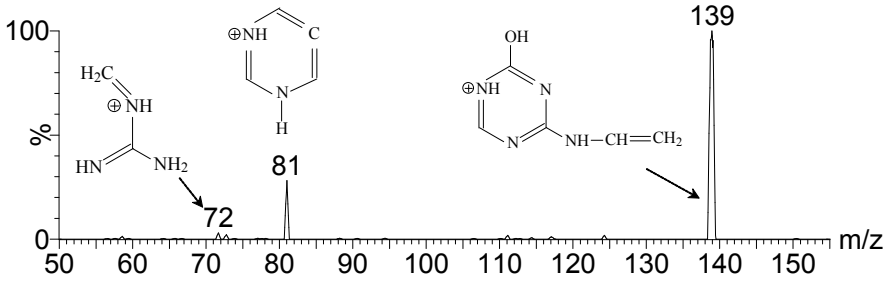

Fig. S14 Molecular structure and MS/MS spectrum of P10 (ESI+, CE=12 eV).

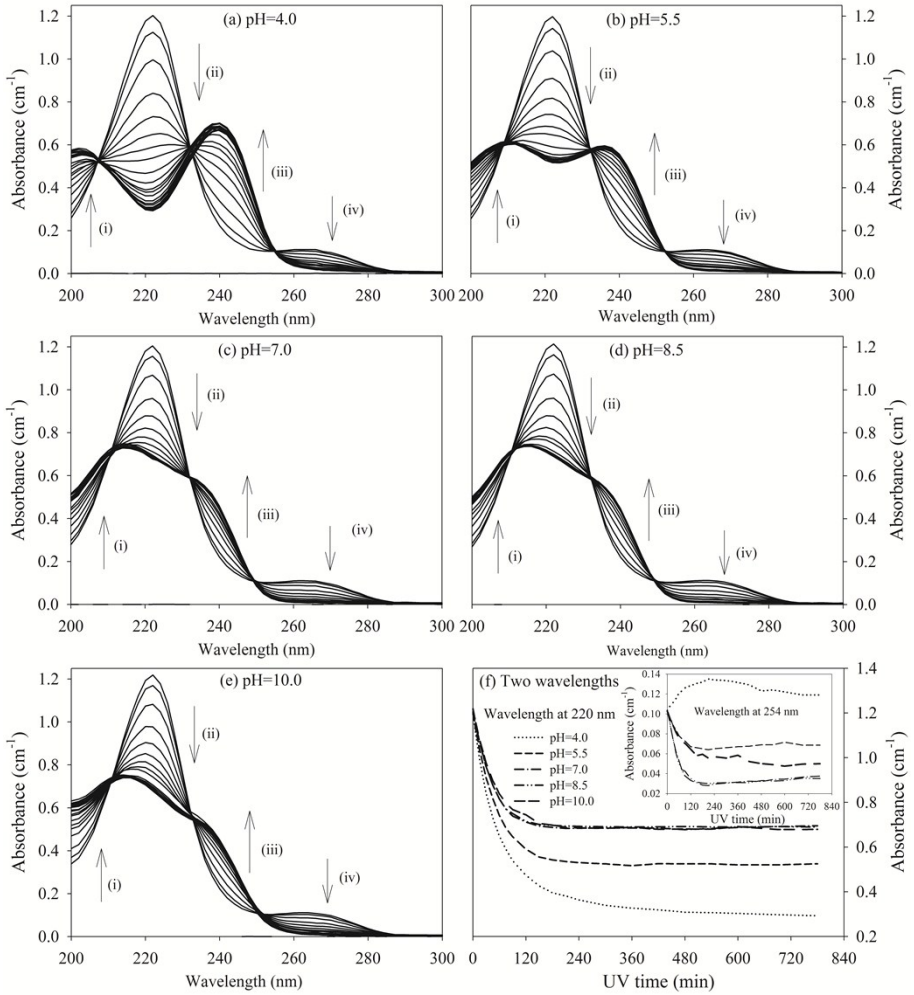

Fig. S15 UV-vis absorbance spectra of ATZ and its products in aqueous solutions at different pH values during sole-UV process.

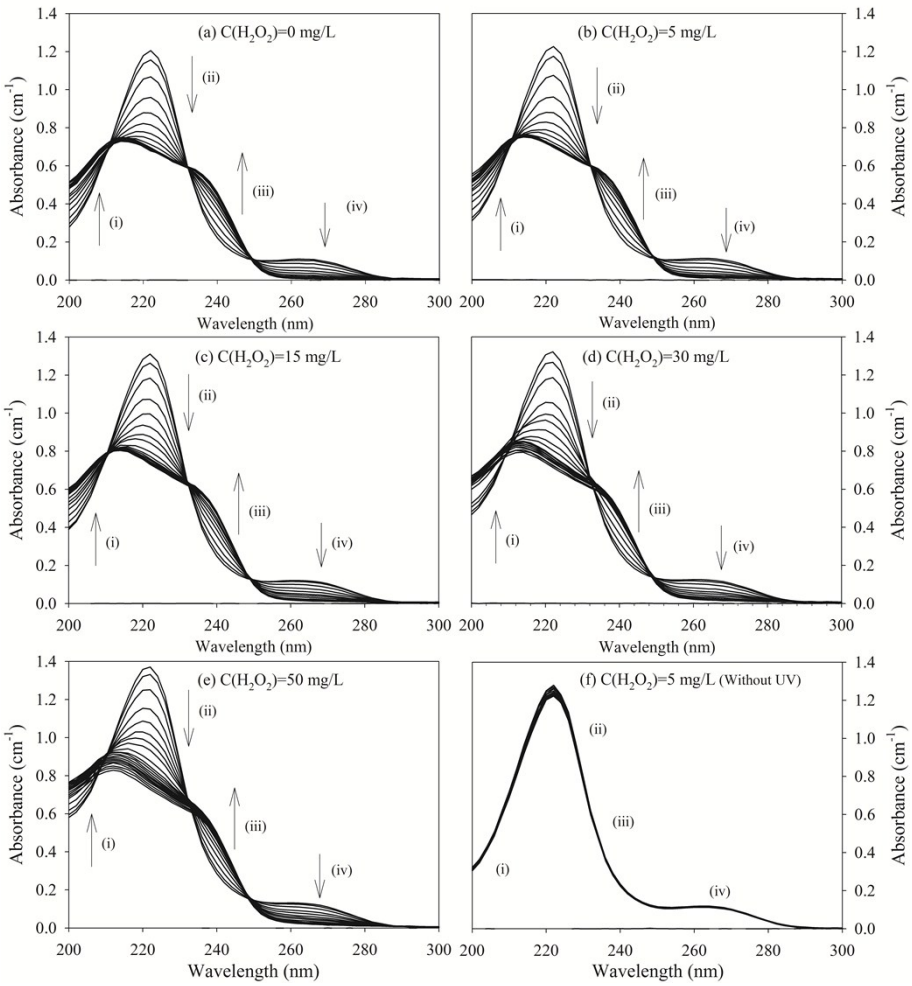

Fig. S16 UV-vis absorbance spectra of ATZ and its products in aqueous solutions at pH of 7.0 during UV/H_2O_2 process.

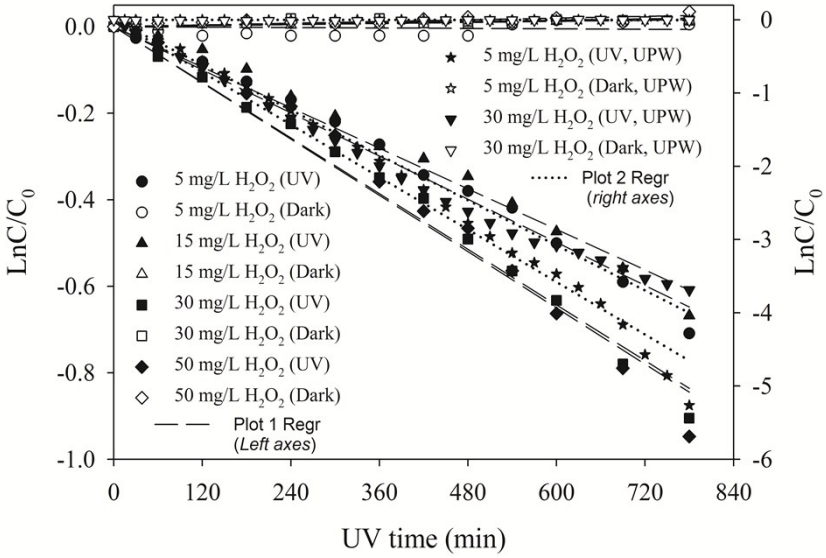

Fig. S17 Degradation of H_2O_2 in UV/H_2O_2 process and the dark controls at pH of 7.0.

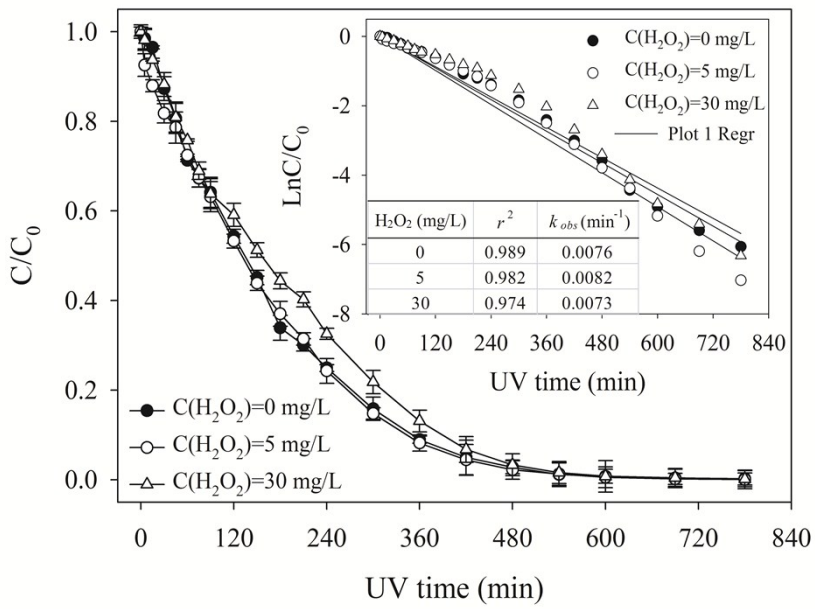

Fig. S18 Effect of H_2O_2 does and irradiation time on degradation of ATZ (5 mg L^{-1}) in aqueous solution at pH of 4.0 during UV irradiation treatment.

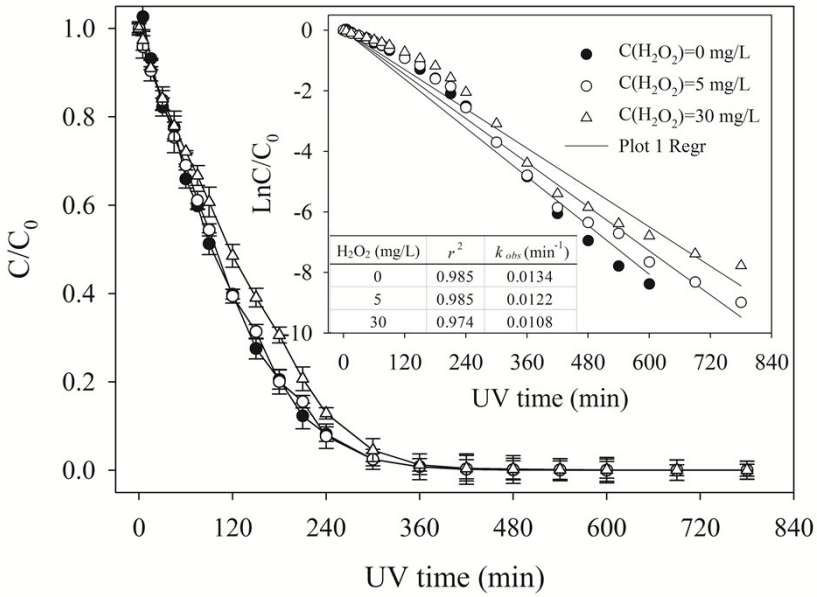

Fig. S19 Effect of H_2O_2 does and irradiation time on degradation of ATZ (5 mg L^{-1}) in aqueous solution at pH of 10.0 during UV irradiation treatment.

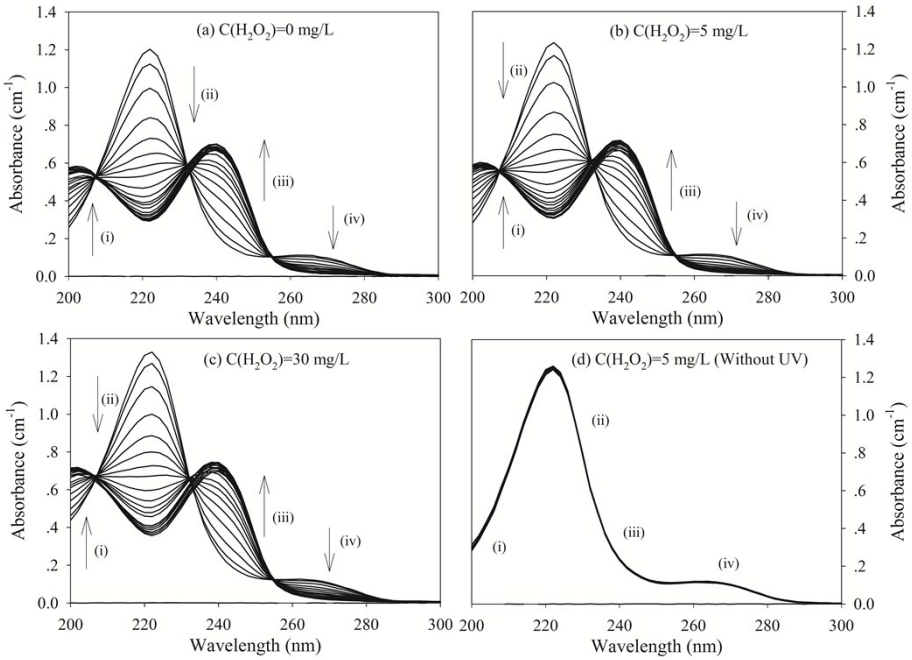

Fig. S20 UV-vis absorbance spectra of ATZ and its products in aqueous solutions at pH of 4.0 during UV/H_2O_2 process.

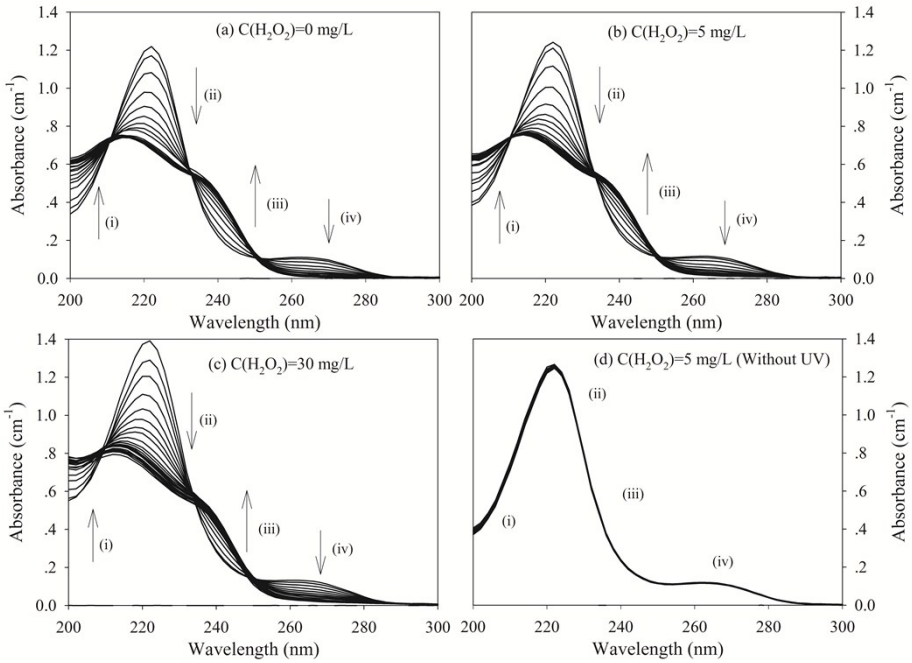

Fig. S21 UV-vis absorbance spectra of ATZ and its products in aqueous solutions at pH of 10.0 during UV/H_2O_2 process.

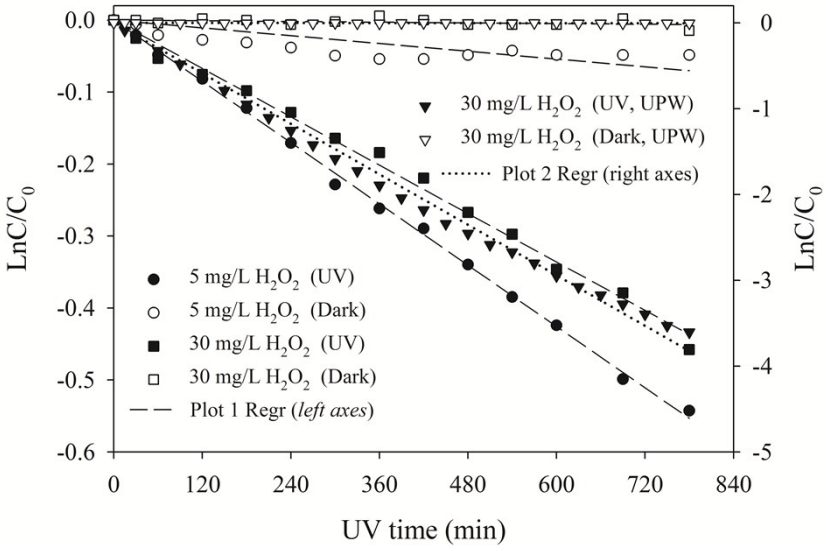

Fig. S22 Degradation of H_2O_2 in UV/H_2O_2 process and the dark controls at pH of 4.0.

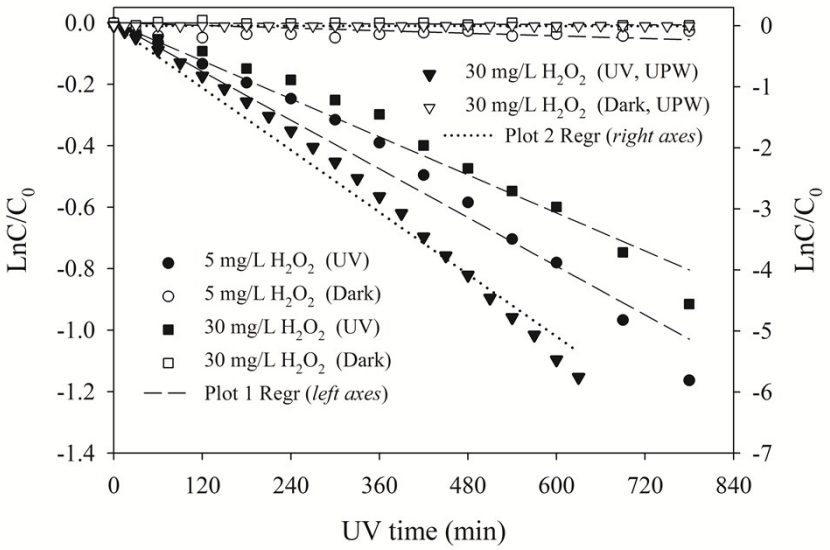

Fig. S23 Degradation of H_2O_2 in UV/H_2O_2 process and the dark controls at pH of 10.0.

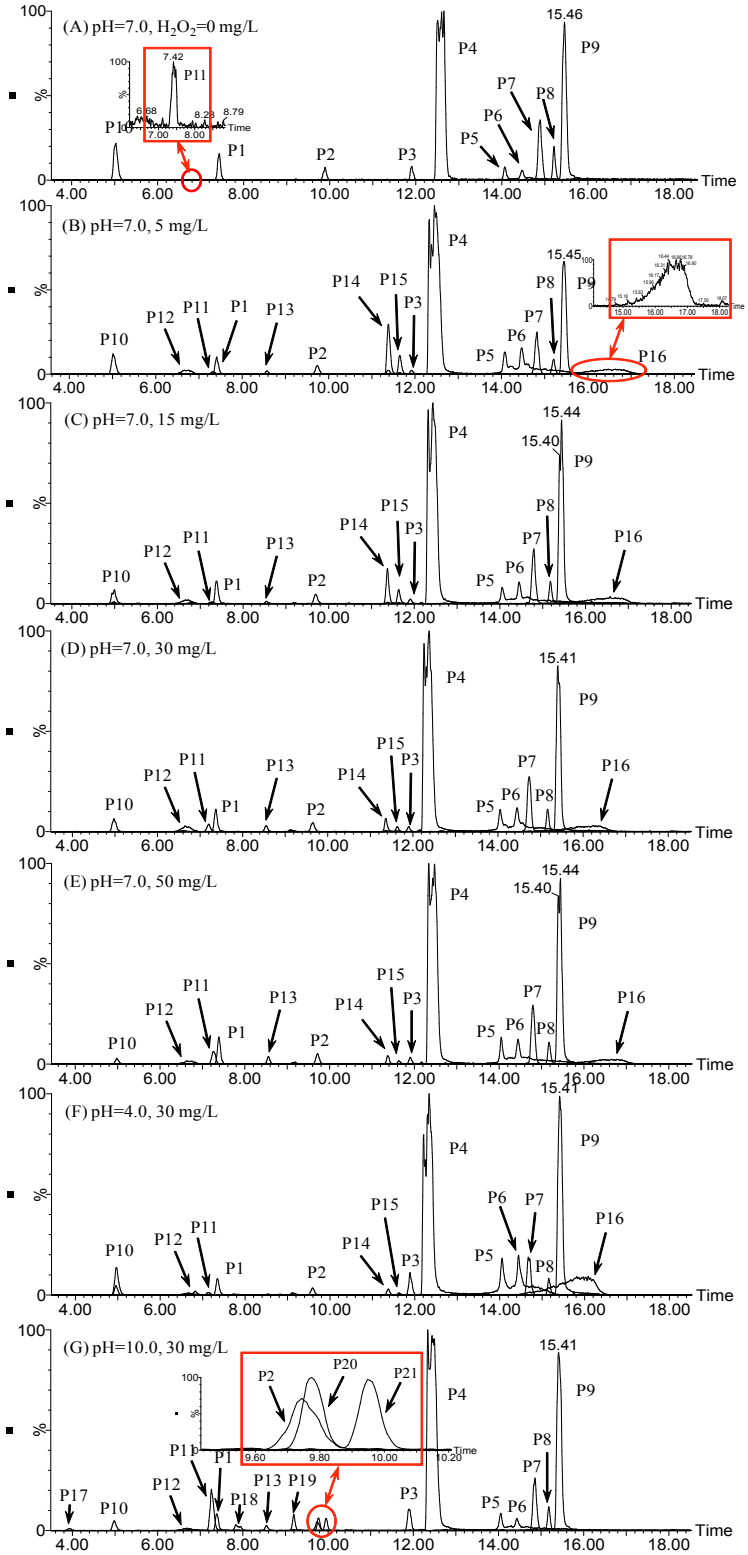

Fig. S24 The EIC of photo-degradation intermediates of ATZ in aqueous solution at 90 min of UV irradiation in UV/H_2O_2 process under different H_2O_2 dose.

(A) pH=7.0, 0 mg L^{-1} H_2O_2; (B) pH=7.0, 5 mg L^{-1} H_2O_2; (C) pH=7.0, 15 mg L^{-1} H_2O_2; (D) pH=7.0, 30 mg L^{-1} H_2O_2; (E) pH=7.0, 50 mg L^{-1} H_2O_2; (F) pH=4.0, 30 mg L^{-1} H_2O_2; (G) pH=10.0, 30 mg L^{-1} H_2O_2.

P12 (2-Hydroxy-4-acetamido-6-isopropenylenylamino-*s*-triazine)

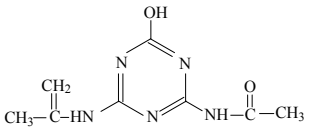

ESI+ mode

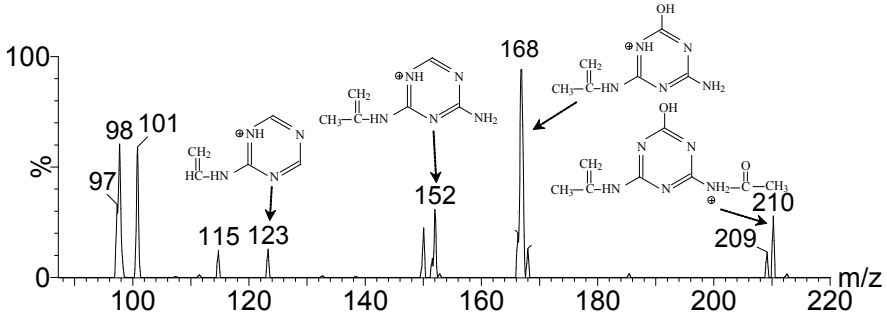

Fig. S25 Molecular structure and MS/MS spectrum of P12 (ESI+, CE=20 eV).

P13 (4-acetamido-*s*-triazine)

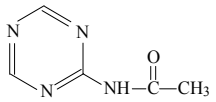

ESI+ mode

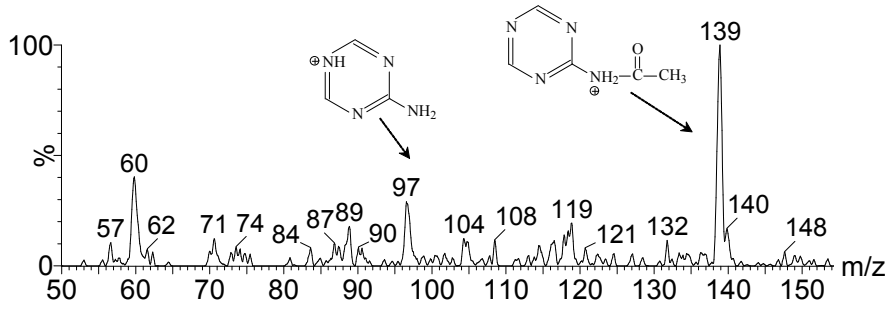

Fig. S26 Molecular structure and MS/MS spectrum of P13 (ESI+, CE=15 eV).

P14 (2-Hydroxy-4-acetamido-6-(2-hydroxyisopropylamino)-*s*-triazine)

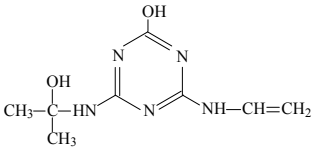

ESI+ mode

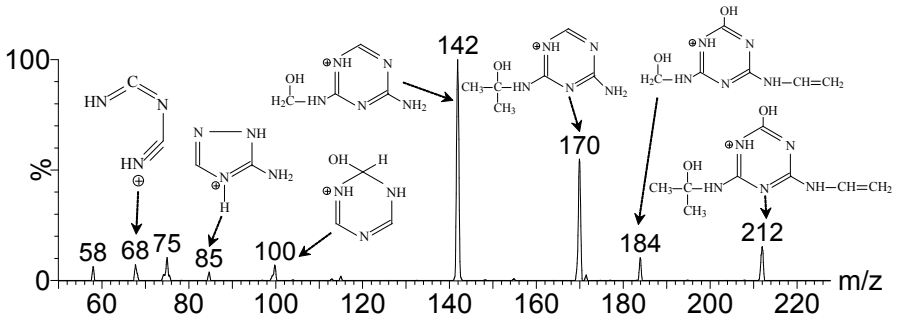

ESI- mode

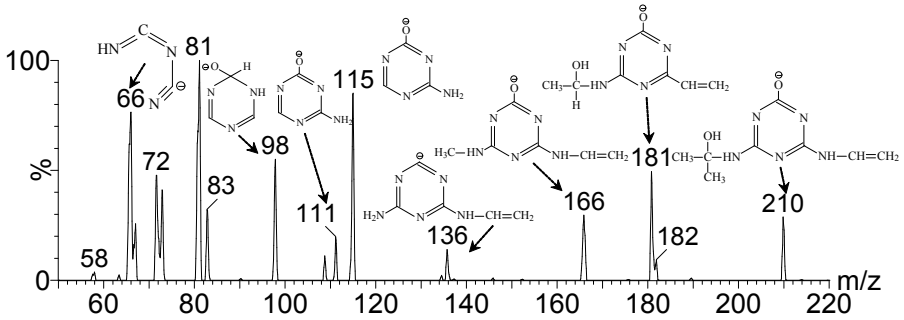

Fig. S27 Molecular structure and MS/MS spectrum of P14 (ESI+ and ESI-, CE=20 eV).

P15 (2-Hydroxy-4-ethylimine-6-(2-hydroxyisopropylamino)-*s*-triazine)

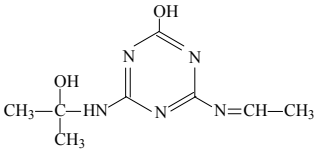

ESI+ mode

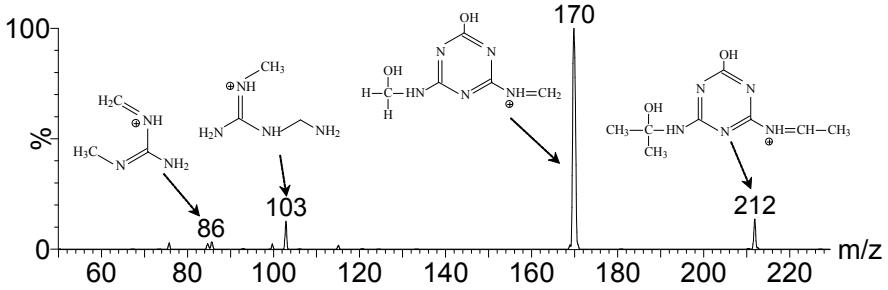

ESI- mode

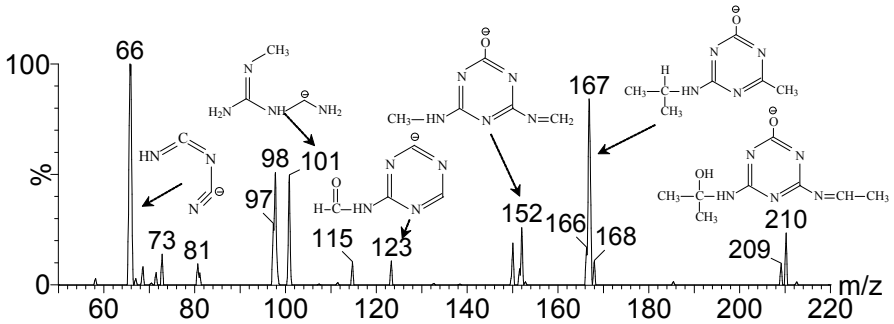

Fig. S28 Molecular structure and MS/MS spectrum of P15 (ESI+ and ESI-, CE=20 eV).

P16 (2-Chloro-4-vinylamino-6-acetamido-*s*-triazine)

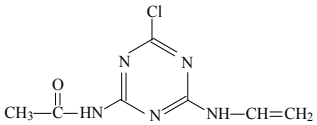

ESI+ mode

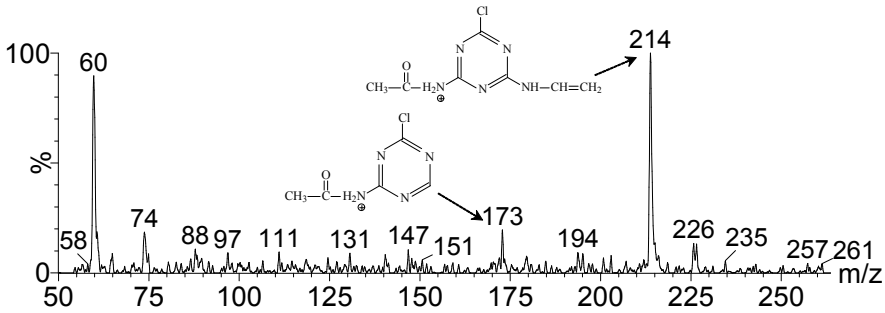

Fig. S29 Molecular structure and MS/MS spectrum of P16 (ESI+, CE=15 eV).

P17 (2-Hydroxy-4-(2-hydroxy-ethylamino)-6-isopropylamino-*s*-striazine)

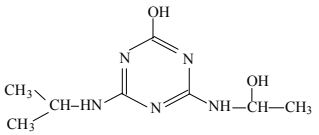

ESI+ mode

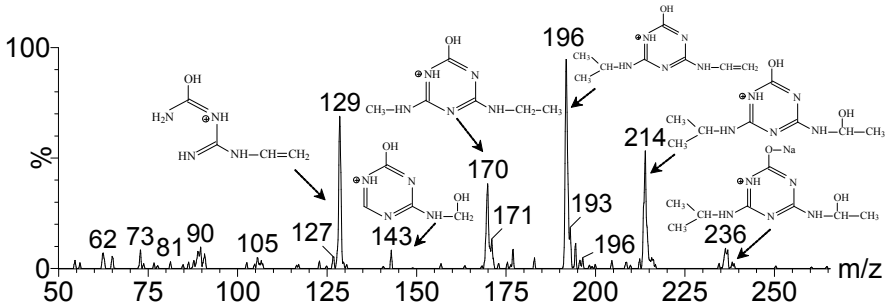

Fig. S30 Molecular structure and MS/MS spectrum of P17 (ESI+, CE=18 eV).

P18 (2-Hydroxy-4-ethylamino-6-(2-hydroxyisopropylamino)-*s*-triazine)

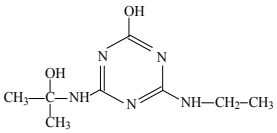

ESI+ mode

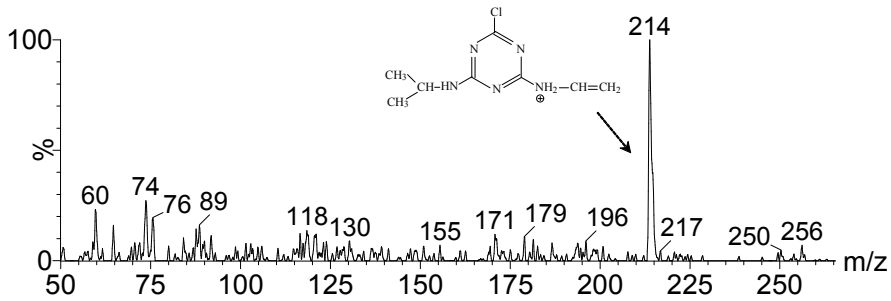

Fig. S31 Molecular structure and MS/MS spectrum of P18 (ESI+, CE=17 eV).

P19 (2-Hydroxy-4-ethylamino-6-isopropenylenylamino-*s*-triazine)

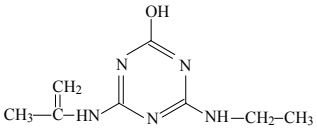

ESI+ mode

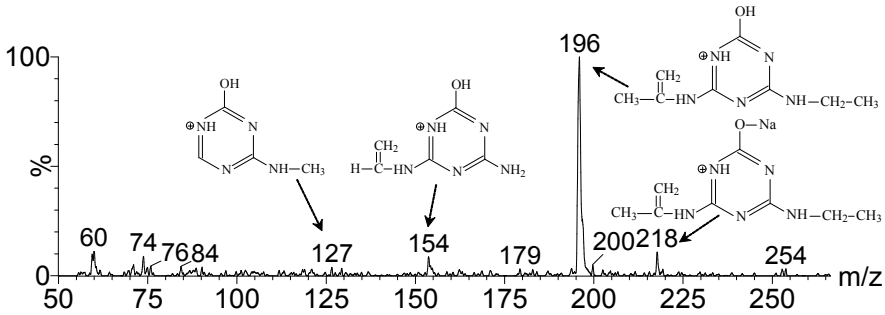

Fig. S32 Molecular structure and MS/MS spectrum of P16 (ESI+, CE=15 eV).

P20 (2-Hydroxy-4-(2-hydroxy-ethylamino)-6-amino-*s*-triazine)

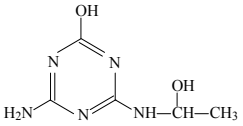

ESI+ mode

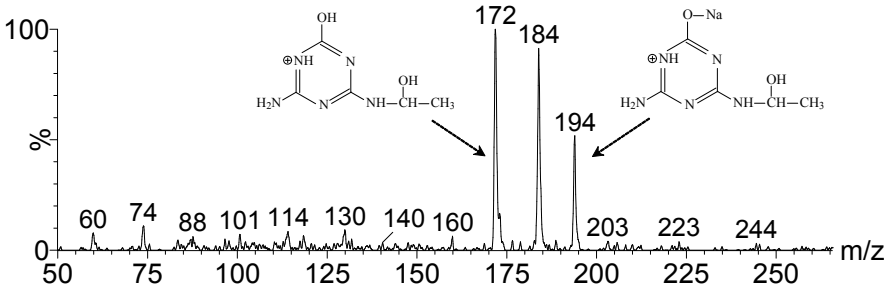

ESI- mode

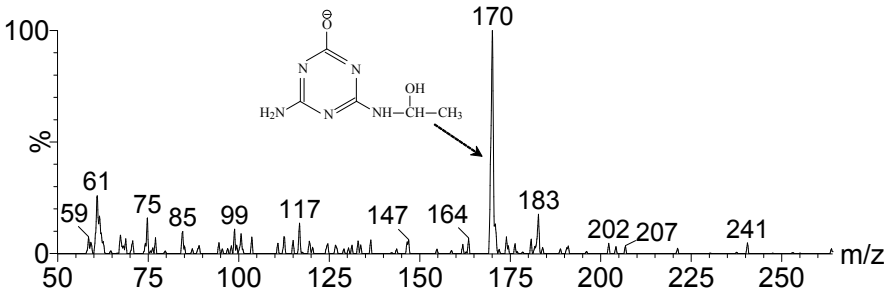

Fig. S33 Molecular structure and MS/MS spectrum of P20 (ESI+ and ESI-, CE=20 eV).

P21 (2-Chloro-4-vinylamino-6-amino-*s*-triazine)

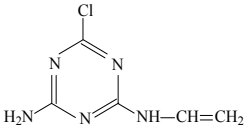

ESI+ mode

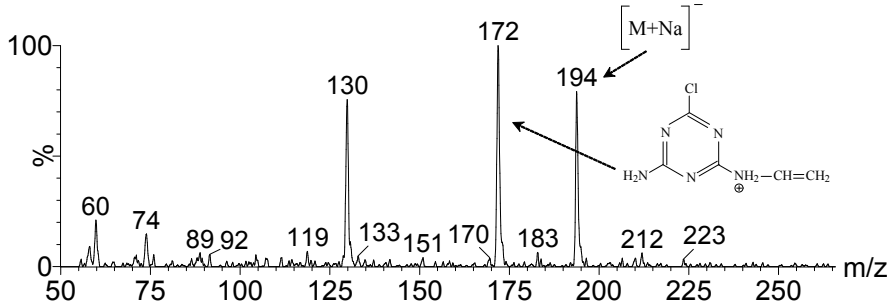

ESI+ mode

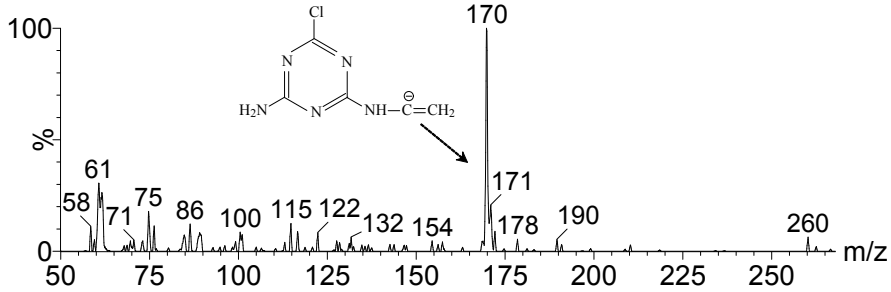

Fig. S34 Molecular structure and MS/MS spectrum of P21 (ESI+ and ESI-, CE=20 eV).

Table S1 Pseudo-first-order reaction rate constants (k_{obs}) of ATZ at different pH values in sole-UV process.

Initial solution pH values	Final solution pH values	Linear correlation coefficient (r^2)	Reaction rate constants k_{obs}（min^{-1}）	Half-life time $t_{1/2}$ (min)
4.0	4.03	0.989	0.0076	91.2
5.5	5.51	0.986	0.0113	61.3
7.0	6.98	0.987	0.0150	46.2
8.5	8.46	0.989	0.0140	49.5
10.0	9.95	0.985	0.0134	51.7

Note: *initial ATZ concentration: 5 mg L^{-1}.*

Table S2 Retention time (RT) and MS spectral information in full scan modes of ATZ and its intermediates.

Name	RT/min	MS spectral (ESI+)	MS spectral (ESI-)
P1	7.42	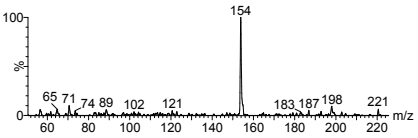	
P2	9.89	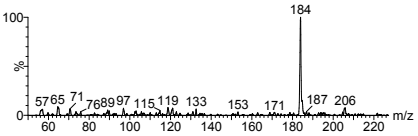	
P3	11.90	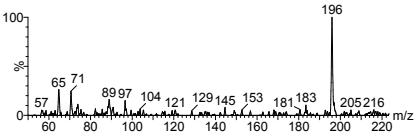	
P4	12.60	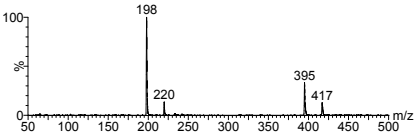	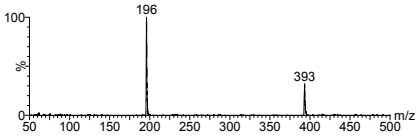
P5	14.06	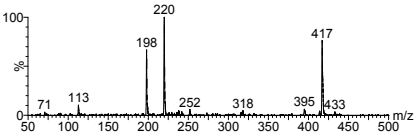	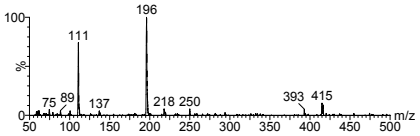
P6	14.46	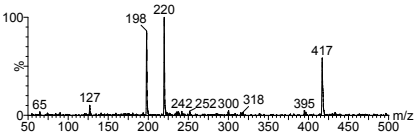	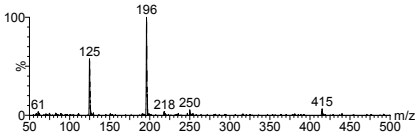
P7	14.88	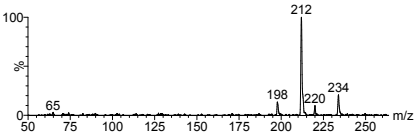	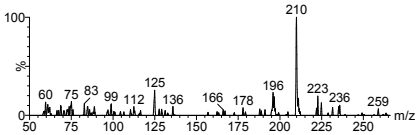
P8	15.20	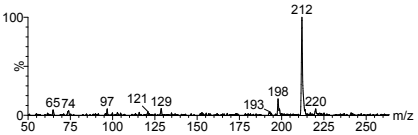	
P9	15.44	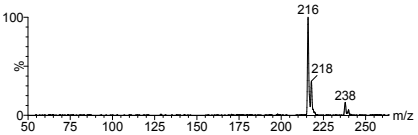	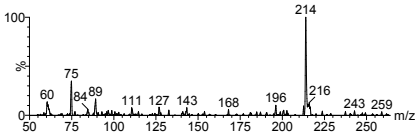
P10	5.02	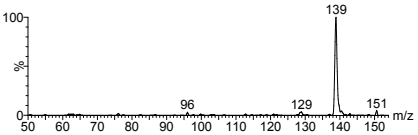	
P11	7.54	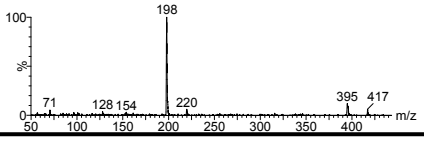	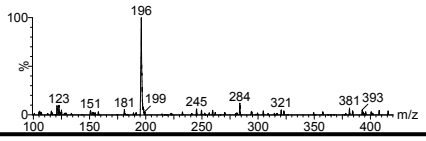

Table S3 Pseudo-first-order reaction rate constants (k_{obs}) of ATZ (initial pH of 7.0) at different H_2O_2 does in UV/H_2O_2 process.

Initial H_2O_2 concentration	Final solution pH values	Linear correlation coefficient (r^2)	Reaction rate constants k_{obs}（min^{-1}）	Half-life time $t_{1/2}$ (min)
0	6.98	0.983	0.0145	46.2
5	6.95	0.979	0.0165	42.0
15	6.88	0.988	0.0118	58.7
30	6.82	0.991	0.0108	64.2
50	6.68	0.995	0.0097	71.5

Table S4 Retention time (RT) and MS spectral information in full scan modes of ATZ and its intermediates.

Name	RT/min	MS spectral (ESI+)	MS spectral (ESI-)
P12	6.70	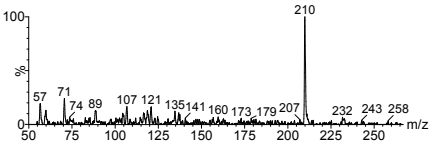	
P13	8.58	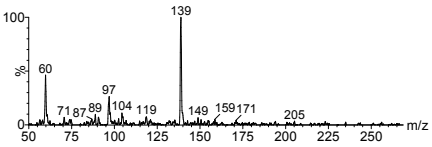	
P14	11.38	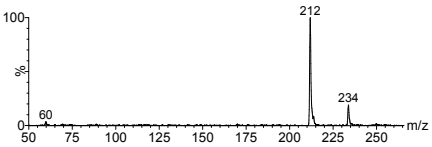	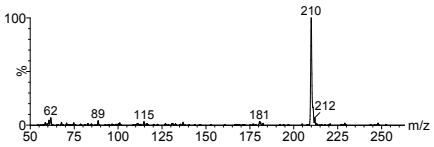
P15	11.64	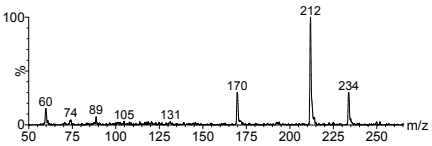	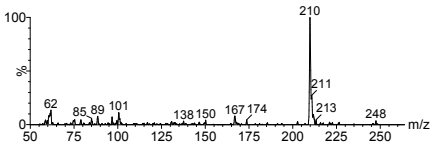
P16	16.60	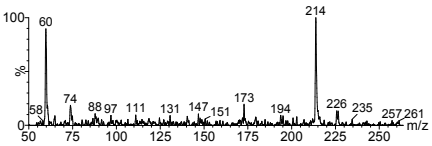	
P17	3.92	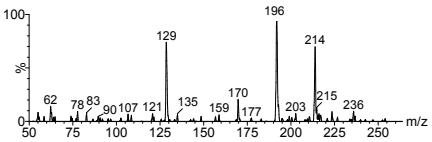	
P18	7.90	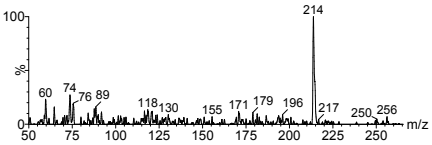	
P19	9.20	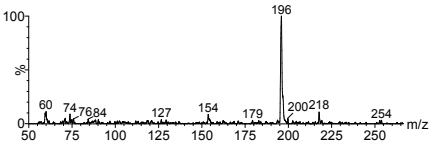	
P20	9.77	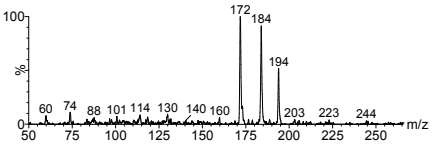	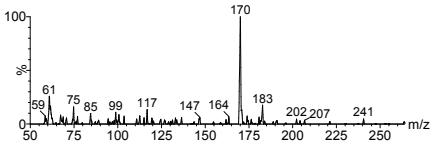
P21	9.95